

Comparative Study of Nonlinear Black-Box Modeling for Power Electronics Converters

2023 IEEE Energy Conversion Congress and Exposition (ECCE) | 979-8-3503-1644-5/23/\$31.00 ©2023 IEEE | DOI: 10.1109/ECCE53617.2023.10362794

Liang Qiao
 Department of Electrical Engineering and
 Computer Science
 The University of Tennessee, Knoxville
 Knoxville, USA
 lqiao1@vols.utk.edu

Yaosuo Xue
 Electrification and Energy Infrastructures
 Division
 Oak Ridge National Laboratory
 Oak Ridge, USA
 xuey@ornl.gov

Yonghao Gui
 Electrification and Energy Infrastructures
 Division
 Oak Ridge National Laboratory
 Oak Ridge, USA
 guiy@ornl.gov

Wei Du
 Electricity Infrastructure and Buildings Division
 Pacific Northwest National Laboratory
 Richland, USA
 wei.du@pnl.gov

Fei (Fred) Wang^{1,2}
¹The University of Tennessee, Knoxville
²Oak Ridge National Laboratory
 Knoxville, USA
 fred.wang@utk.edu

Abstract— With the increasing penetration level of renewable sources and power electronics loads in modern power systems, accurate and computationally efficient models are needed. Black-box model (BBM) could be a useful method in such systems. However, not very extensive research efforts have been made for power electronics BBM so far, and existing works mostly focus on steady-state operation, neglecting the important transient behaviors such as load transients, voltage transients, and faults. This paper presents a comparative study of three commonly used nonlinear BBM approaches for transient behaviors of power electronics converters. Comparison methods are proposed, and the evaluations are conducted under different transients using a grid-connected single-phase photovoltaic inverter. The findings of this study provide valuable references for further feasibility investigations on implementing BBMs in large-scale power electronics-rich power systems.

Keywords—black-box model, data-driven, power electronics, system identification

I. INTRODUCTION

With the rapid growth of inverter-based resources (IBRs) and power electronics interfaced loads in modern power electronics converter (PEC)-rich power systems, models that can accurately represent the inverter dynamic behaviors are essential for system design, operation, and analysis. Modeling challenges arise with such transitions in large-scale power systems, which include the requirement for electro-magnetic transient simulations and accurate PEC models that are suitable for the application of interest [1, 2].

Numerous efforts have been made to develop models that can represent PECs in various contexts. Depending on prior knowledge, there are two different approaches to modeling any dynamic systems: first-principle or knowledge-based modeling and data-driven modeling using empirical data. The former

approach relies on the physics and internal details of a system to mathematically derive the equations for system models. If the system is too complex, derivation of its accurate system model could be complicated. Such knowledge-based models could lead to a huge computation burden for computers. Besides, the internal information of some systems might be confidential or unknown, which makes it impossible to acquire an accurate system model using knowledge-based modeling techniques. Unlike knowledge-based modeling, data-driven modeling uses available data to derive the model that describes the targeted system. This approach assumes that the data contains sufficient information to represent the physics of the targeted systems [3].

The two approaches categorize the modeling process into three types based on the level of information available about the system's parameters and the degree of transparency of the model structure. These categories include white-box, grey-box, and black-box models (BBMs) [4], as shown in Fig. 1 [5].

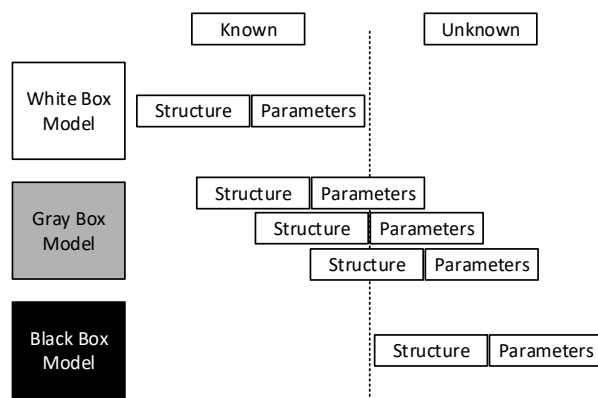


Fig. 1. Categories of dynamical systems by model structure and parameter.

This manuscript has been authored by UT-Battelle, LLC, under contract DE-AC05-00OR22725 with the US Department of Energy (DOE). The US government retains and the publisher, by accepting the article for publication, acknowledges that the US government retains a nonexclusive, paid-up, irrevocable, worldwide license to publish or reproduce the published form of this manuscript, or allow others to do so, for US government purposes. DOE will provide public access to these results of federally sponsored research in accordance with the DOE Public Access Plan (<https://www.energy.gov/doe-public-access-plan>).

For white-box models, both the system structure and its parameters are fully specified. When the structures and parameters are all known, these white-box models can be derived with good accuracy. However, in large-scale PEC-rich systems, PECs are typically provided by different vendors and manufacturers, and detailed internal information is often confidential to system operators or users. Therefore, it is impractical to acquire accurate white-box models for all PECs in a large-scale system. Another issue of detailed white-box models is that they could result in a huge computation burden, especially when they are used for large-scale PEC-rich systems. Accurate white-box models need to incorporate detailed and complex inverter controls, protections, switching actions, hardware characteristics, etc., which could severely slow down the planning and simulation of these large-scale systems. Although efforts have been made to develop more computationally efficient white-box models using linearization and simplification, the application of these models is often limited, and they become inaccurate when large transients are involved. Therefore, white-box models are not appropriate for large-scale system studies due to this limitation.

The gray-box models only partially represent the system structures and/or parameters, with the remainder being unknown or uncertain. This modeling approach has not gained much attention since it still requires part of the system information. It has primarily been utilized for parameter estimation of known topologies [6].

The black-box models, on the other hand, are developed based on empirical data, which means that internal information is not needed to acquire such models. Moreover, they are also computationally efficient once the models are trained. Therefore, such BBMs can be a useful method to solve the aforementioned issues. The BBM approach was initially applied to small-signal modeling of dc-dc converters in an application of spacecraft power systems by Cho starting from the 1980s [7-9]. A black-box model is an abstraction of the model of real-world physics, simply representing the functional relationships between system inputs and outputs without preserving internal physical structure. When a dynamic system is difficult to or cannot be modeled using knowledge-based modeling techniques, system identification methods can be applied to derive its model using the measured system's input and output data. Research of system identification was pioneered by Pieter Eykhoff in the 1960-70s [10], and it is further established with a theoretical framework and practical methodology by Ljung, Soderstrom, and Stoica in the 1980s [11-13]. Fig. 2 illustrates a typical regression-based system identification block diagram.

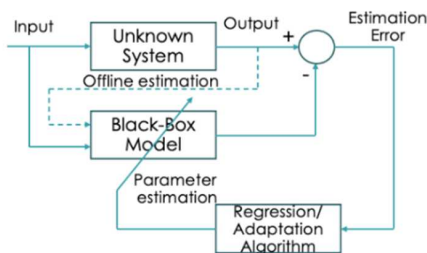


Fig. 2. System identification of an unknown system.

System identification methods can be parametric or non-parametric. Parametric system identification methods involve making assumptions about the functional form of the system's model and estimating the parameters of that model using data. Non-parametric system identification methods, on the other hand, do not require assumptions about the functional form of the system's model, but instead, rely on techniques such as frequency response analysis or spectral analysis to identify the system's characteristics. The parametric model is usually preferred due to its simplicity, less required training data, and fast training speed compared to non-parametric models.

Parametric black-box models take the forms of linear or nonlinear models. The linear models offer a good solution to capture system dynamics at one operating point under small disturbances. Transfer functions (TF), state-space (SS) equations, and autoregressive with exogenous (ARX) are commonly used linear models for PECs [14-16]. However, these models can only represent a system in a small range of a single operating point. For systems with multiple operating points, a polytopic model structure can be utilized [17, 18], which combines multiple small-signal linearized models with weighting factors to achieve a better and compromised solution.

For the systems with nonlinearities and subject to large disturbances like PECs-rich power systems, a nonlinear large-signal model structure shall be adopted. Commonly known nonlinear models used for power electronics applications include:

- 1) Nonlinear AutoRegressive-eXogenous (NARX) model
- 2) Hammerstein-Wiener (HW) model
- 3) Artificial neural networks (ANN) model

Although these BBM approaches have been gradually extended to single-phase and three-phase inverters, not very extensive research efforts have been done for power electronics BBM so far. This paper proposes the comparison method and conduct evaluations for the commonly used nonlinear black-box models for IBR transient modeling. The paper is organized as follows. Section II explains the basic concept of the three nonlinear modeling approaches that are commonly used. In section III, the system under study and the methodology used here are introduced. Section IV provides the results and evaluations of different nonlinear modeling approaches. Conclusions are summarized in Section V.

II. NONLINEAR BLACK-BOX MODELING APPROACHES FOR POWER ELECTRONIC CONVERTERS

A. NARX Model

The NARX model, as shown in Fig. 3, consists of model regressors and one or more mapping objects as the output function. It defines the predicted output $y(t)$ as a function of linear and nonlinear functions of model regressors, together with a fixed offset. The regressors are calculated with the current input $u(t)$ and past input and output data. The regressors in the model can be either linear regressors with delayed inputs and outputs, or they could be nonlinear regressors that incorporate nonlinear functions of delayed inputs and outputs.

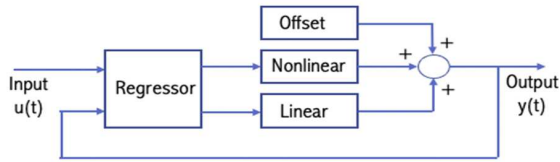


Fig. 3. Model structure of NARX model.

The nonlinear estimator is a sum of linear and nonlinear functions with a fixed offset. The estimator can be described by equation (1) [19], where x represents the vector of the regressors, and r represents the mean of the regressors. $L^T(x - r)$ represents the linear function, $g(Q(x - r))$ represents the nonlinear function, Q is the projection matrix that makes the calculation well-conditioned, and d is a scalar offset.

$$y(t) = L^T(x - r) + g(Q(x - r)) + d \quad (1)$$

In the nonlinear estimator, either the linear or the nonlinear function can be excluded. Possible nonlinear estimators include Sigmoid Network, Wavelet Network, dead-zone, single variable polynomial, saturation, piecewise linear function, tree-partition networks, and multilayer neural networks [20]. Note that in the NARX model, the nonlinear data do not directly impact the linear model, so the nonlinear response cannot be easily tuned in the NARX structure.

B. HW Model

The HW model, as shown in Fig. 4, is a popular approach for the black-box modeling of PECs [21, 22]. In [23], the solar PV inverter is treated as a one-port network and the black-box model takes the form of a voltage-controlled current source implemented in the OpenDSS. It is recognized that the transfer function model cannot capture harmonics, while the HW model can identify up to the 13th-order harmonics [24, 25]. The comparisons between the HW and the NARX model structures have shown that the HW model demonstrates better performance in terms of quality metrics and fit percent [19].

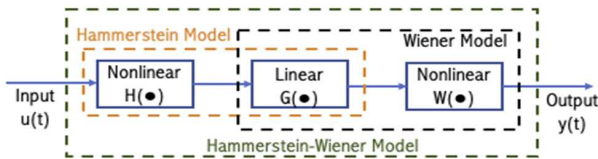


Fig. 4. Model structure of HW model.

The HW model consists of input nonlinear block $H(\cdot)$ and output nonlinear block $W(\cdot)$ in series with a linear block $G(\cdot)$ in the middle. The input and output nonlinear blocks represent the nonlinearities of the input and output, respectively. $H(\cdot)$ is the nonlinear function that transforms the input data $u(t)$, $W(\cdot)$ is the nonlinear function that maps the output of linear block $G(\cdot)$ to the system output $y(t)$. The middle linear block represents the linear transfer function of the system. Similar to the nonlinear estimators in the NARX model, the input and output nonlinearities can also be described as Sigmoid Network, Wavelet Network, saturation, polynomial, dead zone, piecewise

linear function, etc. Note that when the output nonlinear block is not included, the model is called the Hammerstein Model; when the input nonlinear block is not included, the model is then called the Wiener model.

Unlike the NARX model, the linear and nonlinear model responses can be manipulated separately in the HW model, which makes it an effective structure for modeling nonlinear systems like PECs. However, it still faces some challenges to model some complex behaviors as reported in some literature, like the frequency coupling effects [26].

C. ANN Model

The ANN model, which offers desirable solutions in terms of accuracy, has been widely used for system identification as a powerful tool in power electronics applications [27]. The ANN approaches have been attempted to demonstrate their potential for the black-box modeling of PECs in recent years [26, 28, 29]. Neural networks behave similarly to the neural network of the human brain. The basic neural network contains neurons, layers, weights, and activation functions. In a neural network, a "neuron" is a mathematical function that collects and organizes information according to a specific architecture. These neurons can form layers, and the data will be passed through different layers. The input layer will process the input data, while the output layer will provide the output data of the network. Layers between the input layer and the output layer are called hidden layers. The structure of neural networks, the number of neurons and layers, and the activation function can be very different according to different applications. Although neural networks resemble statistical methods such as curve fitting and regression analysis, neural networks are more powerful and can handle more complex tasks due to their ability to learn and adapt from data.

Fig. 5 (a) shows the topology of simple feedforward neural networks (FFNNs). However, as reported in [26], simple FFNNs do not provide the required degree of accuracy when modeling IBRs. Some more advanced topologies, like the nonlinear autoregressive model with exogenous inputs (NARX) neural networks shown in Fig. 5 (b), can provide more accurate predictions in such applications. A general mathematical representation of a NARX NN can be expressed as (2) [26].

$$y(t + 1) = f(u_1(t), \dots, u_n(t), y(t), y(t - D), \dots, y(t - mD)) \quad (2)$$

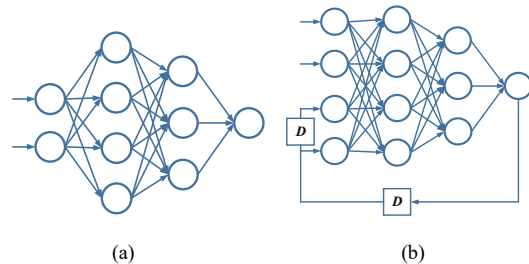


Fig. 5. ANN model structures: (a) FFNN and (b) NARX NN.

It can be seen from equation (2) that the next output value $y(t + 1)$ is a function of n momentary input data u and $m + 1$ past output data y at each time instance t . The discrete time step

D represents the delayed time step, and it depends on the sampling rate f_{sample} of the data. D is described as:

$$D = \frac{1}{f_{sample}} \quad (3)$$

The training of complex ANN models may require lots of data and longtime effort. A large amount of data sets is required and the significant size of neurons at several hundred will likely increase the model complexity and training time. However, once the ANN model is trained, the implemented ANN model will have a reduced computation effort and thus shorter simulation durations compared to the white-box models.

III. CASE STUDY AND METHODOLOGY

A. System Model

In order to evaluate the different nonlinear black-box models and determine the most appropriate modeling approach for large distribution-connected IBRs, a single-phase 240 Vrms, 3500 W grid-connected PV system in MATLAB/Simulink is used for the simulation investigation. The system setup is shown in Fig. 6. The simulation model includes a PV array, a single-phase dc/ac converter with an LCL filter, inverter control, and loads and utility grid. The inverter control has basic functions including an MPPT controller, Vdc regulator, PLL, PWM generator, and voltage/current measurements. The grid-side voltage and current waveforms of the inverter are measured and collected to generate the training and validation data set for the system identifications using three black-box models. TABLE I shows the system parameters of the single-phase PV array.

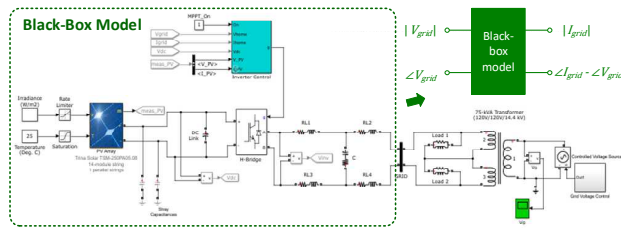


Fig. 6. Single-phase grid-connected PV array.

TABLE I. PARAMETERS OF THE SINGLE-PHASE PV SYSTEM

Electrical Parameters of the Inverter		Values
Nominal Voltage	V_n	240 Vrms
Nominal Power	P_n	3500 W
Frequency	f	60 Hz
Parameters of PV Array		Values
Module	Trina Solar TSM-250PA05.08	
Parallel Strings	1	
Series-connected modules per string	14	
Parameters of Loads		Values
Nominal Voltage	V_{nl}	120 Vrms
Active Power	P_{nl}	5000 W
Inductive Reactive Power	QL_{nl}	5000 var

B. Data Preprocessing

The one-port black-box model is adopted here to evaluate the performance of different modeling approaches. This model has only one port that connects to the grid side. The dynamics of the PV array, the single-phase inverter, and the inverter control will be included in this black-box model. The inverter grid-side voltage is selected as the input of the model, while the inverter grid-side current is selected as the output of the model. Considering the future implementation in the GridLAB-D, the ac signals are transformed into the magnitudes and the phase angles. Eventually, the black-box model is a two-input, two-output model, with the grid voltage magnitude and its phase angle as the model inputs, and the grid current magnitude and the phase angle between voltage and current as the model outputs.

The voltage and current waveforms generated by the simulation need to be preprocessed before using as training and validation data for black-box models. The procedure of the data preprocessing includes:

- Remove start-up data: the data during the start-up process is not needed for the black-box modeling here.
- Correct “bad data”: some of the error data may be generated due to the measurement. These error data need to be correct before the training of black-box models.
- Down sample: the original data set should be down sampled to the lowest acceptable data resolution to reduce the data size and speed up the training and simulation process.
- Rescale: data from different channels should be rescaled between 0 and 1 before the training/validation process.
- Reshape: the format of the original data needs to be reshaped to meet the requirements of black-box models.

C. Training and Validation Data Set

For the black-box system identification of this system, the grid-side voltage and current waveforms are measured, and their magnitudes and phase angles are calculated and collected for the training and validation data set. Two conditions are considered in the training and validation tests: grid voltage perturbation and short-circuit (SC) fault. Fig. 7 (a) and (b) show the input and output data set for model training and validation, respectively. The bottom two figures are the model input signals, while the top two figures are the model output signals. To prevent the model from overfitting, the validation test is different from the training test. In the training test, the grid voltage changed from 1 p.u to 0.95 p.u, 1.05 p.u, 0.9 p.u, and 1.1 p.u, and then falls back to 1 p.u until the short-circuit fault happened. In the validation test, the grid voltage increased from 1 p.u to 1.03 p.u and 1.07 p.u, and then the SC fault happened.

D. Comparison Method

To evaluate the performance of the three black-box modeling approaches, the same training and validation data set, as shown in Fig. 7, are used for the system identification. When comparing the performance of these models, three aspects are considered, which include: 1) model accuracy, 2) model

behaviors (nonlinear behavior characteristics), and 3) model complexity (time).

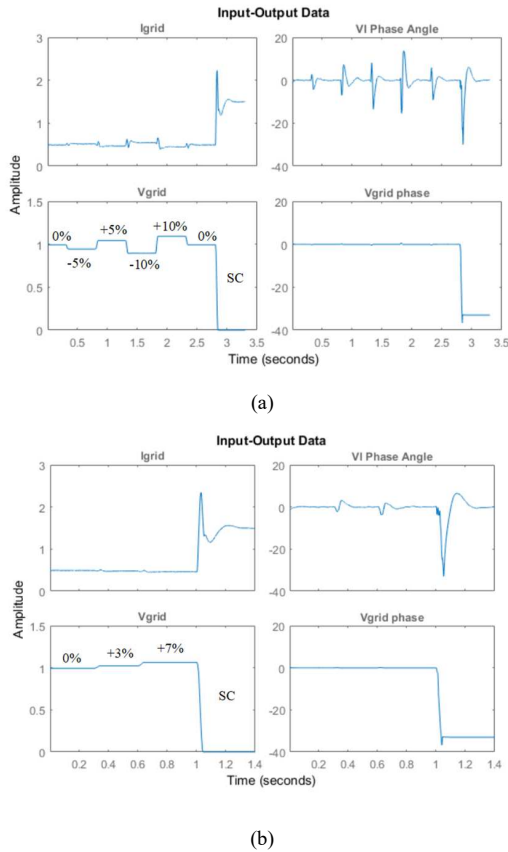


Fig. 7. Training (a) and validation (b) data set.

1) model accuracy

When evaluating the accuracy of different black-box models, the goodness of fit is used as the model quality metric. The goodness of fit returns fit values that represent the error norm between the predicted data of the model and the reference data using a cost function. In this comparison, the normalized root mean squared error (NRMSE) is selected as the cost function. The expression when using NRMSE as the cost function is (4) [30], where $\|$ indicates the 2-norm of a vector. $i = 1, \dots, N$, where N is the number of channels.

$$fit(i) = \frac{\|x_{ref}(:,i) - x(:,i)\|}{\|x_{ref}(:,i) - \text{mean}(x_{ref}(:,i))\|} \quad (4)$$

When the fit value is zero, it indicates a perfect match to reference data; when the fit value is 1, it means that the test data is no better than a straight line at matching the reference data. To calculate the accuracy (in percentage) of each model, (5) is used.

$$accuracy(i) = 100 \left(1 - \frac{\|x_{ref}(:,i) - x(:,i)\|}{\|x_{ref}(:,i) - \text{mean}(x_{ref}(:,i))\|} \right) \quad (5)$$

2) model behaviors

To compare the model behaviors of different black-box models, the nonlinear behavior characterization is used to evaluate if the model can “learn” the nonlinear behaviors of inverters. When designing the training and validation tests, different patterns are designed under multiple inverter transients. These patterns will be used to examine whether the model is suitable for transient modeling applications of PECs.

3) model complexity

When comparing the model complexity of different models, the execution time including both the training and validation process will be considered. A shorter time represents the less computation burden of the model.

IV. RESULTS AND ANALYSIS

Fig. 8 shows the results of three black-box models compared to the simulation results in the validation tests. Fig. 9 and Fig. 10 show the zoom-in view of the grid voltage perturbation behaviors and the short-circuit fault behaviors, respectively. It can be seen that the ANN-based model has the highest accuracy of 97.34% (I_{grid}) and 93.32% (phase angle between voltage and current), followed by 93.01% / 72.28% of the NARX model and 88.51% / 72.42% of the HW model.

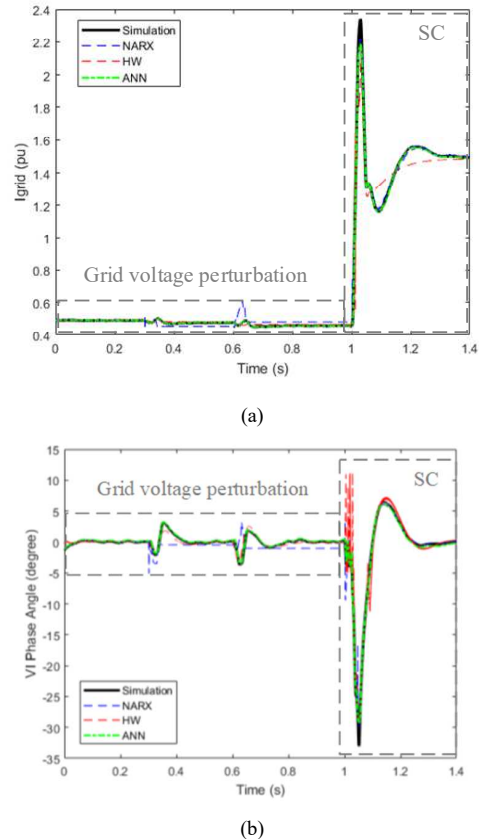


Fig. 8. Comparison of three nonlinear black-box models (NARX, HW, ANN) vs. the simulation results: (a) magnitude and (b) phase angle.

As for the nonlinear behavior characteristics, although the NARX model shows good results for SC fault transient in Fig. 10, the model fails to “learn” the model behavior under the grid

voltage perturbation condition, as shown in Fig. 9. The HW model, as shown in Fig. 9, could predict the trend and steady-state values under the grid voltage perturbation conditions at different perturbation levels, but it shows some errors under the SC fault transient, as shown in Fig. 10.

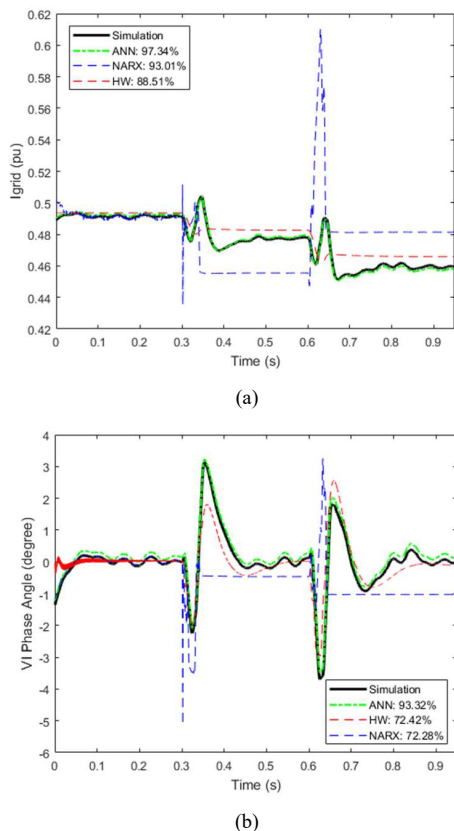


Fig. 9. Zoom-in view of the grid voltage perturbation.

TABLE II shows the execution time of different black-box models. Note that the execution time includes both the training and validation process. With the same training data set, the ANN model provides the best results under both conditions among all three nonlinear models, since it is the only model that can replicate the waveforms under both conditions in the validation test. Not only the trends/patterns and steady-state values at different perturbation levels but also the transient perturbation and fault behaviors are all accurately predicted by the ANN model.

TABLE II. EXECUTION TIME OF THREE BLACK-BOX MODELS

Model	ANN	NARX	HW
Time (s)	8	6	13

Based on the simulation results and comparisons, the ANN-based model structure demonstrates a promising solution and is chosen for the IBR black-box modeling with further optimization, considering its superior performance and manageable model training and implementation efforts. Computation-related performance will be explored in the future under large-scale IBR scenarios.

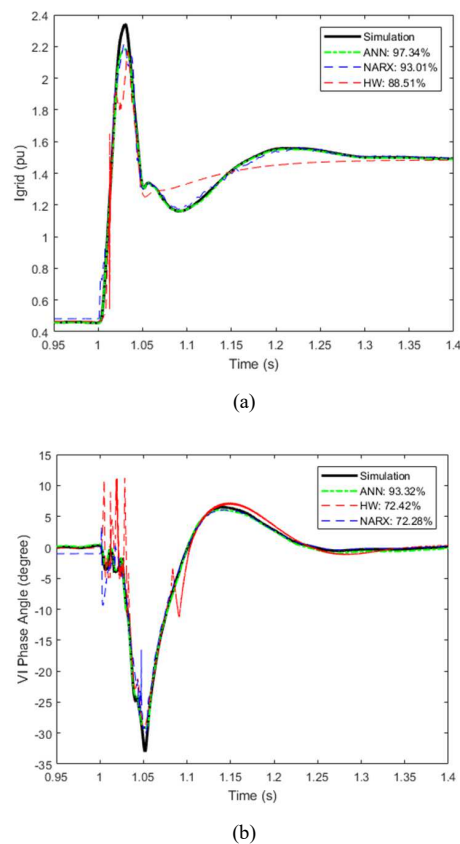


Fig. 10. Zoom-in view of the short-circuit fault.

V. CONCLUSIONS

In this paper, three major nonlinear black-box modeling approaches, including NARX model, HW model, and ANN model, were explored in detail for the modeling of PEC transients. A proposed comparison method was used to compare the model accuracy, model complexity, and nonlinear behavior characterization of the three nonlinear models. These modeling approaches were applied to single-phase solar PV inverters with maximum power-point tracking and standardized control functionalities, which have been modeled as switching models in Matlab/Simulink for acquiring training/validating data sets and performance benchmarking. To evaluate the performance of the models, two transient scenarios were examined, including grid voltage disturbances and grid SC fault. Results indicate that the ANN-based model provides the best model quality and can be considered for future investigation for large-scale distribution-connected IBRs modeling.

ACKNOWLEDGMENT

This material is based upon work supported by the U.S. Department of Energy's Office of Energy Efficiency and Renewable Energy (EERE) under the Solar Energy Technologies Office Award Number 38453. This work also made use of Engineering Research Center Shared Facilities provided by the Engineering Research Center Program of the National Science Foundation and the Department of Energy

under NSF Award Number EEC1041877 and the CURENT Industry Partnership Program.

Abridged Legal Disclaimer: The views expressed herein do not necessarily represent the views of the U.S. Department of Energy or the United States Government.

REFERENCES

- [1] C. Shah, J. D. Vasquez-Plaza, D. D. Campo-Ossa, J. F. Patarroyo-Montenegro, N. Guruwacharya, N. Bhujel, R. D. Trevizan, F. A. Rengifo, M. Shirazi, and R. Tonkoski, "Review of dynamic and transient modeling of power electronic converters for converter dominated power systems," *IEEE Access*, vol. 9, pp. 82094-82117, 2021.
- [2] L. Kong, Y. Xue, L. Qiao, and F. Wang, "Review of Small-Signal Converter-Driven Stability Issues in Power Systems," *IEEE Open Access Journal of Power and Energy*, vol. 9, pp. 29-41, 2022.
- [3] D. P. Solomatine and A. Ostfeld, "Data-driven modelling: some past experiences and new approaches," *Journal of hydroinformatics*, vol. 10, no. 1, pp. 3-22, 2008.
- [4] J. Sjöberg, Q. Zhang, L. Ljung, A. Benveniste, B. Delyon, P.-Y. Glorennec, H. Hjalmarsson, and A. Juditsky, "Nonlinear black-box modeling in system identification: a unified overview," *Automatica*, vol. 31, no. 12, pp. 1691-1724, 1995.
- [5] A. Alqahtani, M. Alsaffar, M. El-Sayed, and B. Alajmi, "Data-driven photovoltaic system modeling based on nonlinear system identification," *International Journal of Photoenergy*, vol. 2016, 2016.
- [6] B. H. Lin, J. T. Tsai, and K. L. Lian, "A non-invasive method for estimating circuit and control parameters of voltage source converters," *IEEE Transactions on Circuits and Systems I: Regular Papers*, vol. 66, no. 12, pp. 4911-4921, 2019.
- [7] B. H. Cho, MODELING AND ANALYSIS OF SPACECRAFT POWER SYSTEMS (SOLAR, SHUNT, SWITCHING, STABILITY). Virginia Polytechnic Institute and State University, 1985.
- [8] B. H. Cho and F. C. Y. Lee, "Modeling and analysis of spacecraft power systems," *IEEE Transactions on Power Electronics*, vol. 3, no. 1, pp. 44-54, 1988.
- [9] J.-Y. Choi, B. H. Cho, H. F. VanLandingham, H.-s. Mok, and J.-H. Song, "System identification of power converters based on a black-box approach," *IEEE Transactions on Circuits and Systems I: Fundamental Theory and Applications*, vol. 45, no. 11, pp. 1148-1158, 1998.
- [10] P. Eykhoff, *System identification*. Wiley London, 1974.
- [11] L. Ljung, *System identification*. Springer, 1998.
- [12] L. Ljung and T. Söderström, *Theory and practice of recursive identification*. MIT press, 1983.
- [13] T. Söderström and P. Stoica, *System identification*. Prentice-Hall International, 1989.
- [14] N. Guruwacharya, N. Bhujel, U. Tamrakar, M. Rauniar, S. Subedi, S. E. Berg, T. M. Hansen, and R. Tonkoski, "Data-driven power electronic converter modeling for low inertia power system dynamic studies," in *IEEE Power & Energy Society General Meeting (PESGM)*, 2020: IEEE, pp. 1-5.
- [15] I. Cvetkovic, D. Boroyevich, R. Burgos, and Z. Liu, "Generalized Behavioral Models of Three-Phase Converters and Electric Machines for System-Level Study and Stability Assessment," in *IEEE 11th International Symposium on Power Electronics for Distributed Generation Systems (PEDG)*: IEEE, pp. 291-296.
- [16] A. Naziris, A. Frances, R. Asensi, and J. Uceda, "Black-box small-signal structure for single-phase and three-phase electric vehicle battery chargers," *IEEE Access*, vol. 8, pp. 170496-170506, 2020.
- [17] G. Guarderas, A. Frances, D. Ramirez, R. Asensi, and J. Uceda, "Blackbox large-signal modeling of grid-connected DC-AC electronic power converters," *Energies*, vol. 12, no. 6, p. 989, 2019.
- [18] V. Valdivia, A. Lazaro, A. Barrado, P. Zumel, C. Fernandez, and M. Sanz, "Black-box modeling of three-phase voltage source inverters for system-level analysis," *IEEE Transactions on Industrial Electronics*, vol. 59, no. 9, pp. 3648-3662, 2011.
- [19] N. Patcharaprakiti, K. Kirtikara, D. Chenvidhya, V. Monyakul, and B. Muenpinij, "Modeling of single phase inverter of photovoltaic system using system identification," in *Second International Conference on Computer and Network Technology*, 2010: IEEE, pp. 462-466.
- [20] L. Wieserman, "Developing a Transient Photovoltaic Inverter Model in OpenDSS Using the Hammerstein-Wiener Mathematical Structure," University of Pittsburgh, 2017.
- [21] N. Patcharaprakiti, K. Kirtikara, V. Monyakul, D. Chenvidhya, J. Thongpron, A. Sangswang, and B. Muenpinij, "Modeling of single phase inverter of photovoltaic system using Hammerstein-Wiener nonlinear system identification," *Current Applied Physics*, vol. 10, no. 3, pp. S532-S536, 2010.
- [22] N. Patcharaprakiti, K. Kirtikara, K. Tunlasakun, J. Thongpron, D. Chenvidhya, A. Sangswang, V. Monyakul, and B. Muenpinij, "Modeling of photovoltaic grid connected inverters based on nonlinear system identification for power quality analysis," *Electrical Generation and Distribution Systems and Power Quality Disturbances*, pp. 53-82, 2011.
- [23] L. M. Wieserman, S. Graziani, T. E. McDermott, R. C. Dugan, and Z.-H. Mao, "Test-Based Modeling of Photovoltaic Inverter Impact on Distribution Systems," in *IEEE Photovoltaic Specialists Conference (PVSC)*, 2019: IEEE, pp. 2977-2983.
- [24] A. S. Abdelsamad, J. M. A. Myrzik, E. Kaufhold, J. Meyer, and P. Schegner, "Voltage-Source Converter Harmonic Characteristic Modeling Using Hammerstein-Wiener Approach," *IEEE Canadian Journal of Electrical and Computer Engineering*, vol. 44, no. 4, pp. 402-410, 2021.
- [25] A. S. Abdelsamad, M. J. Myrzik, E. Kaufhold, J. Meyer, and P. Schegner, "Nonlinear identification approach for black-box modeling of voltage source converter harmonic characteristics," in *IEEE Electric Power and Energy Conference (EPEC)*, 2020: IEEE, pp. 1-5.
- [26] E. Kaufhold, S. Grandl, J. Meyer, and P. Schegner, "Feasibility of black-box time domain modeling of single-phase photovoltaic inverters using artificial neural networks," *Energies*, vol. 14, no. 8, p. 2118, 2021.
- [27] S. Zhao, F. Blaabjerg, and H. Wang, "An overview of artificial intelligence applications for power electronics," *IEEE Transactions on Power Electronics*, vol. 36, no. 4, pp. 4633-4658, 2020.
- [28] H. D. Abbood and A. Benigni, "Data-driven modeling of a commercial photovoltaic microinverter," *Modelling and Simulation in Engineering*, vol. 2018, 2018.
- [29] M. Stender, O. Wallscheid, and J. Böcker, "Comparison of Gray-Box and Black-Box Two-Level Three-Phase Inverter Models for Electrical Drives," *IEEE Transactions on Industrial Electronics*, vol. 68, no. 9, pp. 8646-8656, 2021.
- [30] MathWorks. "goodnessOfFit." <https://www.mathworks.com/help/ident/ref/goodnessoffit.html> (accessed 03/27/2023).